PRELIMINARY DOSIMETRIC EVALUATION OF ELECTRON SOURCE TERMS AT PW LASER SYSTEMS

Maria-Ana POPOVICI[1], Romeo IONICA[2], Gh. CATA-DANIL[3]

Recent advances in laser technology gave rise to an increasing number of ultrahigh intensity laser facilities. Their operation makes the requirements for radiation protection measures as stringent as those inherent in conventional particle accelerators. Sources of ionizing radiation at a PW laser system can be more diverse and more hazardous, as theory and particle-in-cell (PIC) simulations of laser driven particle acceleration foresee. This paper presents a Monte Carlo simulation approach to the problem of radiation protection associated with PW laser induced electron sources. FLUKA and GEANT4 codes were used to calculate doses due to selected electron source terms. They can be obtained with any ultrahigh power laser and represent the starting points in the radioprotection design/verifying. Our evalution includes absorbed doses and energetic spectra of the secondary particles.

Keywords: PW lasers, radiation protection, Monte Carlo simulation, FLUKA, GEANT4, dose evaluation.

1. Introduction

Petawatt-class laser systems provide ultrashort, ultrahigh intensity laser pulses. Worldwide there are still few facilities where such lasers are in operation or under construction, e.g. Berkeley Lab Laser Accelerator – BELLA and Texas Petawatt Laser in USA, RAL Vulcan and Astra-Gemini in UK, POLARIS and PHELIX in Germany, PETAL and LULLI in France, CAEP, China, J-KAREN, Japan, etc. In Romania, the 1PW CETAL laser was completed in 2014. Romania is also a partner in the most ambitious project concerning multi-PW laser systems, Extreme Light Infrastructure. At the Romanian pillar, ELI – Nuclear Physics (ELI-NP), a 2 x 10 PW laser system will be operating in 2016. A short review of the main scientific subjects to be approached at ELI-NP is given in Ref. [1].

[1] Lecturer , Physics Dept., University POLITEHNICA of Bucharest, Romania, email: popovici@physics.pub.ro
[2] Lecturer , Physics Dept., University POLITEHNICA of Bucharest, Romania, email: r_ionica@physics.pub.ro
[3] Prof., Physics Dept., University POLITEHNICA of Bucharest, Romania, email: cata-danil@physics.pub.ro

In the ultrahigh intensity laser light - matter interaction theoretical and experimental studies revealed a significant production of ionizing radiation. The type of radiation and its spatial and temporal properties depend both on the characteristics of the laser pulse and on the selected laser target [2]. Consequently, the activity at ultrahigh intensity laser facilities is associated to a radiological risk which needs to be permanently evaluated and monitored.

Any such evaluation relies on the "source term", meaning the type and the amount of ionizing radiation, its energy spectrum and spatial distribution. At an ultrahigh intensity laser facility such as CETAL or ELI-NP (to mention only those which will operate in Romania), a large variety of experiments will be performed, resulting in emissions of electrons, photons, protons, neutrons, muons, etc., either as primary particles or as secondaries [3]. Primary radiation will comprise electrons, photons, protons or heavy ions, with electrons playing the leading role. Because they are light charged particles, electrons are the first to react to the huge electric fields in the laser pulse. Their behaviour will eventually determine the structure of the complex radiation fields at the site of a laser – target interaction. This is why in this preliminary study we focus on electrons, particularly hot, relativistic ones, which are generated when incident intensities exceed the relativistic threshold of $10^{18}\ \mathrm{W/cm^2}$ [4].

The goal of this study is to determine doses due to selected electron sources as a starting point for a complex Monte Carlo radiological characterization of a more realistic experimental site. We took into consideration the case of ultrahigh relativistic intensities which are expected with PW and multi-PW laser systems like CETAL and ELI-NP. We also had in view a preliminary cross-check of the FLUKA and GEANT4 simulations results.

2. Electron source terms

The worst radiological electron source terms are expected in laser – plasma acceleration experiments. There are several mechanisms that generate hot electrons by a very efficient energetic transfer between the ultrahigh intensity laser pulse and the plasma which is instantaneously created by the pulse pedestal when it is incident on the target. The most important are i) laser wakefield acceleration (LWFA) with its particular self – modulated (SM-LWFA) and blow-out/bubble regimes [5], [6] and ii) direct laser accelelation (DLA) in plasma channels [7].

The electron source terms we selected do not fit into the category of ideally monoenergetic, monodirectional beams. These represent the ultimate goal of laser acceleration but there are still few experimental results of this type, to our knowledge [8]. Moreover, radiation protection and shielding of such sources are

well established due to currently vast experience with conventional electron accelerators. Instead, we worked with more or less broader energetic and spatial distributions that may be obtained (according to PIC simulations and scaling laws) or even were determined in current experiments.

Source Term 1 (ST1) is a Gaussian energy distribution with a relatively large width:

$$\frac{\mathrm{d}N}{\mathrm{d}E} = \frac{2\sqrt{\ln 2/\pi}}{\Delta E} N_0 \exp\left[-4\ln 2 \frac{\left(E - E_{\mathrm{av}}\right)^2}{\left(\Delta E\right)^2}\right] \tag{1}$$

where $N(E)\mathrm{d}E$ is the total number of electrons per sr, per pulse, in $[E, E+\mathrm{d}E]$, ΔE is the FWHM of the distribution and N_0 - the number of electrons per sr, per pulse for all energies. The average electron energy E_{av} was identified to the energy gain given by the scaling law [9]:

$$E_{\mathrm{av}}[\mathrm{GeV}] \approx 1.7\left(\frac{P[\mathrm{TW}]}{100}\right)^{1/3}\left(\frac{10^{18}}{n_{\mathrm{e}}\left[\mathrm{cm}^{-3}\right]}\right)^{2/3}\left(\frac{0.8}{\lambda_{\mathrm{L}}[\mu\mathrm{m}]}\right), \tag{2}$$

where P is the laser power, n_{e} - the electron plasma density and λ_{L} - the laser wavelength. Eq. (2) describes the energy gain of electrons accelerated in the bubble regime of the LWFA. By using the parameters of a laser delivering 10 PW beam at $0.840\ \mu\mathrm{m}$ wavelength, which propagates in an underdense plasma of density $n_{\mathrm{e}} = 10^{17}\,\mathrm{cm}^{-3}$, we estimated a 34 GeV Gaussian distribution with a relative spread $\Delta E/E = 10\%$, as PIC simulations suggest [10]. The divergence of the implemented source was 3°.

The scaling laws also include a total number of accelerated electrons per laser pulse which is proportional to $P^{1/2}$:

$$N \approx 2.5\cdot 10^9 \frac{\lambda_{\mathrm{L}}[\mu\mathrm{m}]}{0.8}\left(\frac{P[\mathrm{TW}]}{100}\right)^{1/2} \tag{3}$$

Source Term 2 (ST2) and Source Term 3 (ST3) are based on experimental results of electron laser acceleration in overdense plasma obtained at SLAC, RAL Vulcan and LULLI [11], [12], [13], [14]. The electron energetic spectrum is approximated by a relativistic Maxwell – Boltzmann distribution [11]:

$$\frac{\mathrm{d}N}{\mathrm{d}E} = \frac{6.24 \cdot 10^{12} \cdot W_{\mathrm{e}}}{6T_{\mathrm{h}}^4} E^2 \exp\left[-\frac{E}{T_{\mathrm{h}}}\right] \tag{4}$$

where W_{e} is the total energy of the electrons (a fraction of laser pulse energy), and T_{h} is the hot electron temperature in MeV. The latter was calculated according to the scaling law:

$$T_{\mathrm{h}} = 0.511\mathrm{MeV}\left(\sqrt{1.0 + \frac{I_{\mathrm{L}} \cdot \lambda_{\mathrm{L}}^2}{1.37 \cdot 10^{18}}} - 1.0\right) \tag{5}$$

where I_{L} is the laser intensity in $\mathrm{W/cm^2}$.

ST2 is the result of sampling the energy distribution (4) with $T_{\mathrm{h}} = 116$ MeV which corresponds to a laser intensity $I_{\mathrm{L}} = 10^{23}$ $\mathrm{W/cm^2}$ and a wavelength of 0.840 μm. The spatial distribution was considered isotropic, a situation which is close to some experimental observations [14].

ST3 describes experimental results in which the laser target is solid and it is not completely ionized by the laser pulse (thick target experiments). The electron energetic spectrum is similar to ST2. We simulated the electron beam as a pencil beam originating close to the front face of the 2 mm thick, 2mm radius, cylindrical laser target in gold.

ST4 is a superposition of two exponential distributions retrieved from experimental data measured at RAL Vulcan in helium gas jet target. The estimations were given in the final document of ELI – Preparatory Phase [15]:

$$\frac{\mathrm{d}N}{\mathrm{d}E} = \frac{N_1}{T_1}\exp\left(-E/T_1\right) + \frac{N_2}{T_2}\exp\left(-E/T_2\right) \tag{6}$$

The total number of electrons per sr per pulse N_i and the temperature T_i of each thermal component are presented in the table below together with the cutoff energy. The contribution of the second Boltzmannian term is about 16% electron primaries in the range 100MeV-300MeV.

Parameters of ST4

Cutoff energy $E_{\max}$ (MeV)	Temperature T_i (MeV)		Particle number N_i ($\mathrm{sr^{-1}pulse^{-1}}$)	
300	17.6	3500	2.8×10^{9}	1.0×10^{10}

3. Simulation Setup

The doses due to our choice of electron source terms were obtained by parallel FLUKA and GEANT4 calculations. Both codes are Monte Carlo based but FLUKA is a fully integrated physics package, while GEANT4 is a toolkit software. They are widely used simulation tools in dosimetry.

The present Fluka simulations were carried out with the latest published version, FLUKA 2011.2c.0 and Flair 2.0-5 [16, 17, 18]. The 34 GeV Gaussian electron distribution with a 10% relative spread (ST1) was defined by FLUKA BEAM card. ST2 and ST3 were implemented by SOURCE subroutines which sampled the relativistic Maxwellian energy distribution - Eq. (4). For the isotropic ST2, the primary electron direction was sampled from a random (θ,φ) uniform distribution in a 4π sr solid angle. ST3 was defined as a pencil beam. The double exponential source term was generated by a dedicated SOURCE subroutine. Electrons whose energies were sampled from Eq. (6) were generated in a proportion given by the ratio of the overall number of electrons per pulse in the components, N_2/N_1. The spatial distribution was uniform in azimuth and polar angles, within a cone whose aperture is given by the full divergence angle of the beam.

The secondaries were produced and transported with a threshold which was 100 keV for e+/e- and 10 keV for all the other particles, except neutrons which were transported down to the smallest thermal energy, $10^{-5}\,\mathrm{eV}$. In FLUKA, if an interaction generates a particle whose energy is below the production/transport threshold, the particle is not generated but its energy is deposited. Full "heavy" ion transport was activated. To improve the statistics in sampling photonuclear reactions, the inelastic interaction length of photons was reduced by a factor 0.02. This common biasing technique is necessary since their cross sections are much smaller than those of electromagnetic processes.

The GEANT4 simulations were performed with 10.00.p02 version of the toolkit [19]. The dose was accumulated directly from energy deposition at each step in the selected volume. As physics models we have adopted prepackaged physics list QBBC (with default threshold of 0.7mm). Calculations with various physics lists used in studies of shielding applications (QGSP_BERT_HP, QGSP_BIC_HP, QGSP_INCLXX, Shielding) did not lead to appreciable results differences on absorbed physical dose. The various spectral and angular distributions of initial particles were sampled using General Particle Source (GPS) module implemented in GEANT4 distribution.

In Fig. 1 the simplified geometry of our simulations is presented. It consists of a $1.3\text{m (width)} \times 1.4\text{m (height)} \times 2.8\text{m (length)}$ vacuum interaction chamber in the surrounding air. The walls are 6cm thick, in aluminum. Outside the interaction chamber, 1m away from its window, a cube in copper of side 10cm is placed. This is the "detector" where doses due to the electron source placed in the center of the interaction chamber are computed. Copper was selected because it is a material which is likely to be found in a laser interaction bunker, either as a component of a beamdump or some experimental apparatus.

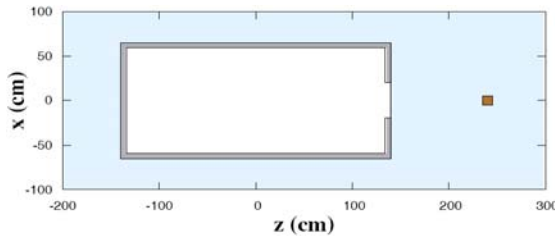

Fig. 1. Simulation geometry

We also calculated the dose in the walls of the interaction chamber and its window. The window geometry (cylindrical, 20 cm radius and 1 mm thick) was chosen so that it does not drastically change the primary electron spectrum. Its large size is designed to allow more electron primaries to leave the interaction chamber, when they have a large spatial distribution (ST2).

4. Results

The main outcome of this study concerns doses calculated by FLUKA and GEANT4 Monte Carlo transport codes. In Table 1 total doses absorbed in the key elements of the geometry: "detector" copper cube, interaction chamber walls and chamber window are presented together with the statistical relative errors. The simulation results compare well. They are, with two exceptions, within the limits of statistical errors.

The "all particles" fluence distribution generated by ST1 is represented in Fig. 2. It is determined by the highly energetic primary electron beam and its very narrow divergence. We notice a forward peaked distribution which is enhanced by the processes that take place in the "detector" region. The 6 cm thick aluminum interaction chamber makes the fluence behind it insignificant. In this simulation 37% of the primary energy is used in electromagnetic cascades, which give rise to an important number of photons, (many of which are bremsstrahlung radiation in aluminum and copper) and electrons covering a wide energy range (Fig.3a).

Table 1. Dose (pGy/primary) due to all particles generated by the implemented electron source terms and associated relative errors (%)

		Source Term 1 Dose (pGy/primary)	Source Term 2 Dose (pGy/primary)	Source Term 3 Dose (pGy/primary)	Source Term 4 Dose (pGy/primary)
Detector	FLUKA	2.2798E + 02 ±0.04%	6.7158E – 04 ±4.3%	1.7932 ±0.06%	1.3473 ±0.04%
	GEANT4	2.2843E + 02 ±0.07%	6.8485E – 04 ±2.98%	1.7934 ±0.02%	0.4740 ±0.07%
Interaction chamber	FLUKA	2.1436E – 04 ±0.47%	2.9711E – 03 ±0.01%	6.3466E – 04 ±0.04%	6.3545E – 06 ±0.02%
	GEANT4	2.3917E – 04 ±0.42%	2.964E – 03 ±0.54%	6.294E – 04 ±0.05%	3.077E – 06 ±0.02%
Window	FLUKA	1.9658E – 01 ±0.42%	1.0535E – 03 ±0.54%	1.8614E – 01 ±0.03%	1.9633E – 01 ±0.01%
	GEANT4	1.9798E – 01 ±0.13%	1.0554E – 03 ±0.47%	1.8539E – 01 ±0.05%	2.017E – 01 ±0.01%

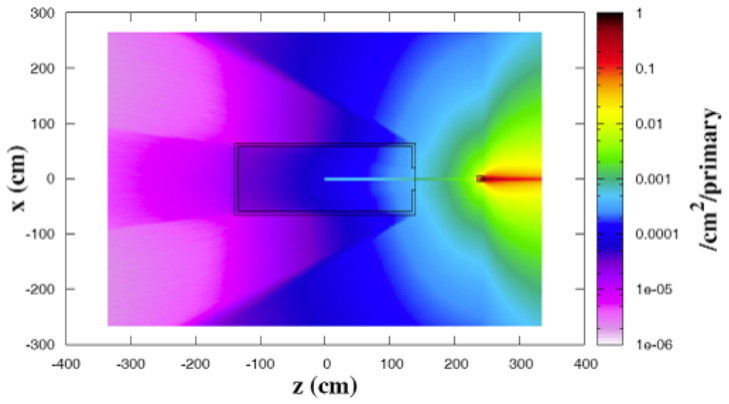

Fig. 2. All particle fluence (particles/cm^2/primary electron) generated by ST1 in the Oxz plane at y= 0. The small divergence source is placed at the center of the interaction chamber

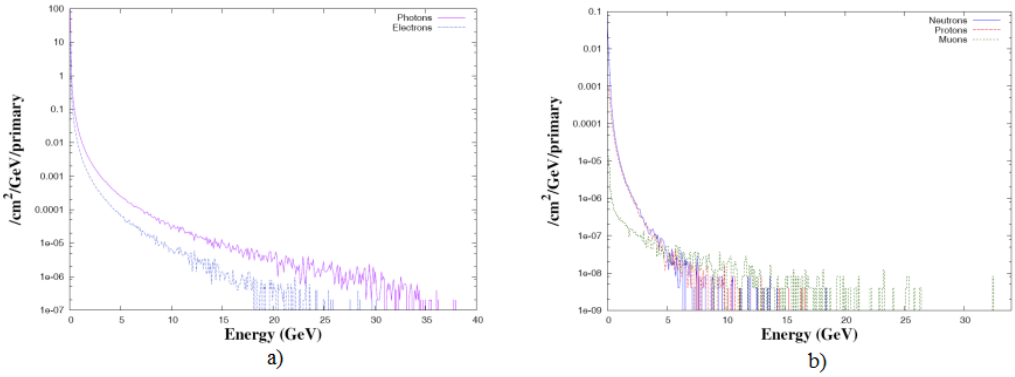

Fig. 3. ST1 - Secondary energy spectra at the front face of the "detector " region, in the backward direction. a) electrons & photons; b) neutrons, protons & muons

Due to the large number of photons that get into the detector region and whose energy is above 0.01 GeV, neutrons are produced in giant resonance and quasi-deuteron photonuclear reactions (see Fig. 3b). They are responsible for the isotropic fluence distribution around the detector region. Highly energetic photons also produce other nuclear reactions giving rise to forward peaked cascade neutrons but also pions (positive, negative and neutral) which decay to muons which represent a problem type of particles in shielding.

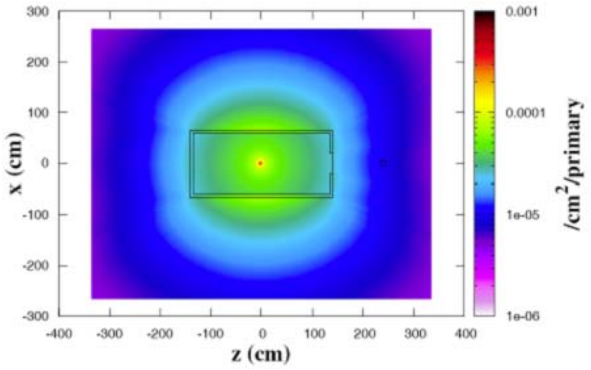

Fig. 4. All particle fluence (particles/cm^2/primary electron) generated by ST2 in the Oxz plane at y = 0. The isotropic source is placed at the center of the interaction chamber

In fact 95% of the stars produced in this simulation were photon induced and only 3% were neutron induced.

If we look at the numbers, ST2 is less hazardous (the maximum electron energy being 1.2 GeV, the averagy energy – 0.350 GeV, i.e. approximately $3T_h$) and closer to the electron distributions that are currently obtained at the PW laser

sites. As expected, the fluence distribution is radially symmetrical inside the vacuum interaction chamber. Cascading of the primary electrons in the thick chamber walls gives more radiation in the environmental air (Fig. 4).

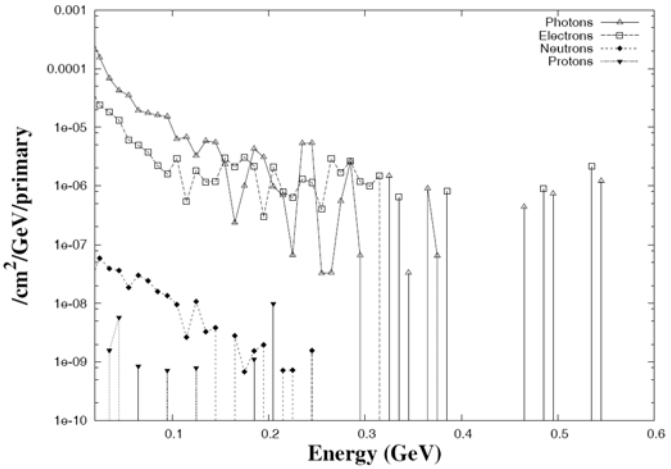

Fig. 5. ST2 - Secondary particles energy spectra at the front face of the "detector " region, in the backward direction

In Fig. 5 we can see the energy spectra of the main secondary particles obtained at the air / copper interface. The isotropic direction of primary electrons and the small solid angle under which electrons get into the "detector" region make the number of nuclear interactions taking place there significantly low. Again, the main particles responsible for nuclear interactions are photons (96.4%). 16% of the primary electron energy is found in GeV electromagnetic cascades and practically no hadronic cascades are produced. High energy photons induce nuclear reactions, thus giving neutrons, protons and even muons, but their fluence is small.

The same energetic distribution of primary electrons will give an altogether different radiation field if the divergence of the beam is extremely low, as in ST3. The fluence due to all particles, depicted in Fig. 6, exhibits an expected forward peaked distribution and a correspondingly good shielding given by the interaction chamber in the backward direction. The interaction of the hot electrons with the gold thick target generates secondaries whose fluence is observed inside the vacuum chamber (please compare to Fig. 2). 34.6% of the incident energy per primary can be found in the electromagnetic cascades in gold, aluminum and copper. According to figure 7, an important number of photons with energies above 0.01 GeV are produced in the detector region. They will induce photo-nuclear and photo-pion reaction, thus generating neutrons, protons and pions. The

largest fraction of muons is obtained by decaying of π^0. Most of the secondaries generated in inelastic interactions are photons (66%) and neutrons (26%) per incident electron primary.

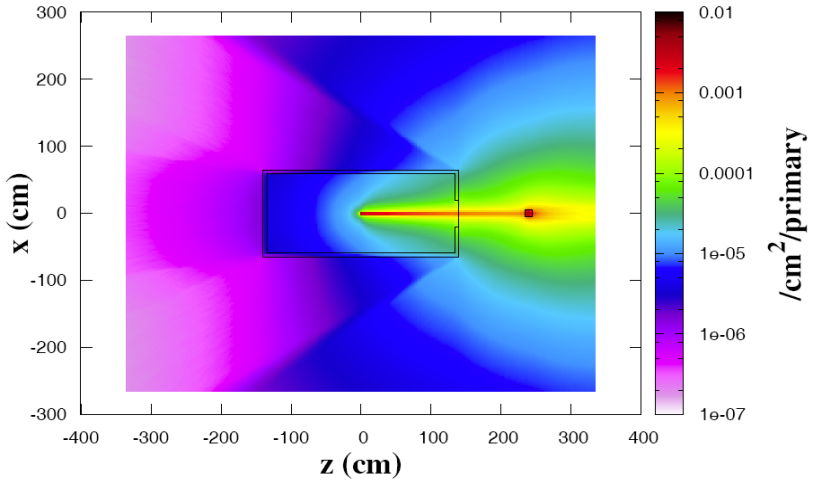

Fig. 6. All particle fluence (particles/cm^2/primary electron) generated by ST3 in the Oxz plane at y = 0. The pencil beam source is placed in front of the laser target, at the center of the interaction chamber

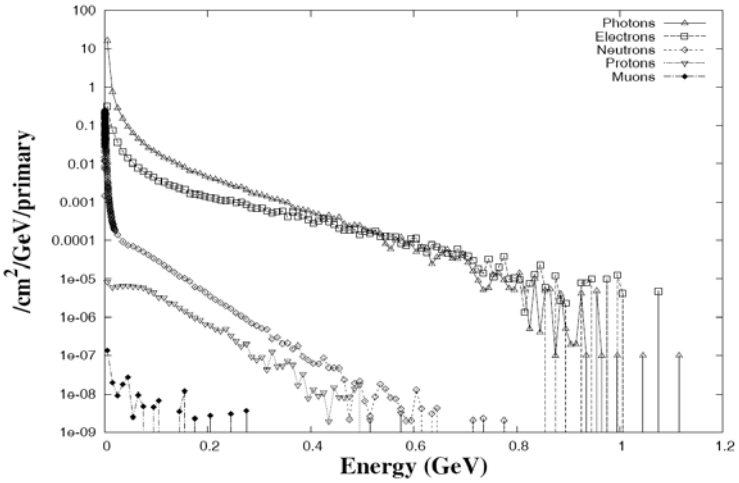

Fig. 7. ST3 - Secondary particles energy spectra at the front face of the "detector " region, in the backward direction

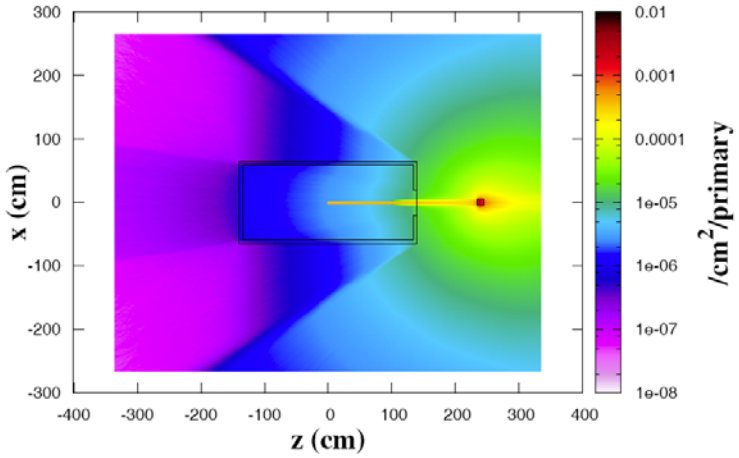

Fig. 8. All particle fluence (particles/cm^2/primary electron) generated by ST4 in the Oxz plane at y = 0. The isotropic source is placed at the center of the interaction chamber

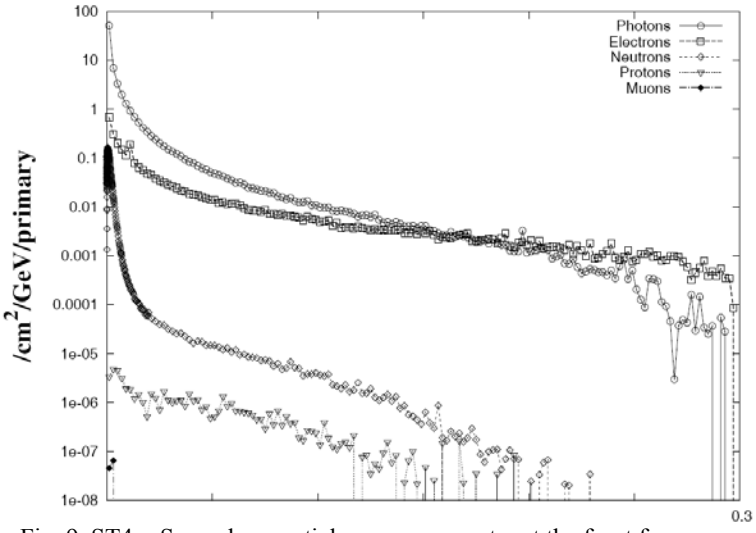

Fig. 9. ST4 - Secondary particles energy spectra at the front face of the "detector " region, in the backward direction

ST4 is a source term which was obtained by modelling real experimental data. The cutoff at 0.300 GeV makes it the least difficult source term from the

radioprotection point of view. However it produces an important fluence of secondary particles around the detector region. It was the only source term for which we obtained back-reflected primaries at the air – copper interface of the detector region and at the window, as you can notice by comparing Fig. 8 to Figs. 2, 4 and 6. Fig. 9 shows that electromagnetic cascades are again the most significant sources of secondaries in the ST4 case. Even more so, since 64% of the incident energy per primary is to be found there. High energetic photons induce nuclear reactions which result in a significant number of neutrons and protons. Muons are not important here.

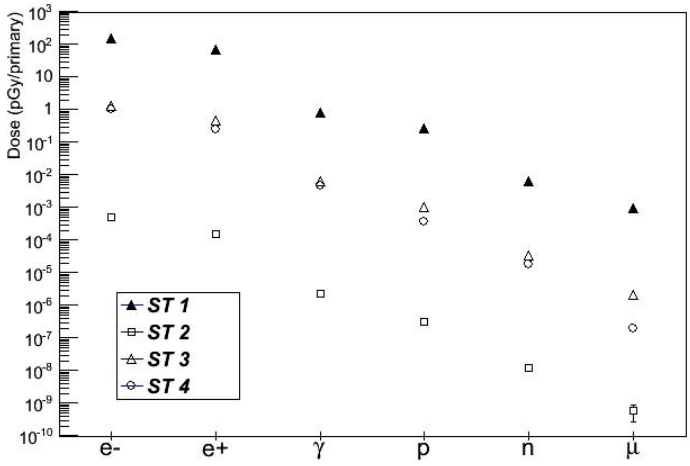

Fig. 10. All particle dose (pGy/primary electron) due to the electron source terms in the "Detector " region.

Finally, in Fig. 10, a comparative graph representation of doses (pGy/primary) due to secondary particles generated by our choice of electron source terms is presented. We emphasize that the dose deposited in the "detector" region is mainly due to the interactions of the defined electron source in that region. The simplified geometry reduces to a minimum the influence of the environment. However, in a real bunker, the radiation fields would be drastically changed by the shielding and any other existing item.

As expected, the highest doses were due to the relatively wide gaussian energy distribution of an electron beam with low divergence. There are roughly six orders magnitudes between the doses due to the "worst" (from a radiprotection point of view) and the "easiest" electron source terms, ST1 and ST2. ST3 and ST4 give very close results due to an energy *range* which is similar (although the energy distributions are obviously quite different), and low divergence. If it had

not been for the nuclear interactions of the electron beam inside the laser target, the results would have been even closer.

From an energetic point of view, ST2 is identical with ST3, but due to its isotropic spatial distribution, it will generate a significantly lower dose in the "detector" region. Obviously this is just a re-distribution of the total energy in the primary beam and for this reason interaction chambers usually have thick walls and can be fitted with suplementary local shielding.

5. Conclusions

This is a Monte Carlo simulation study meant to give a dosimetric evaluation of several typical electron sources at ultrahigh intensity laser facilities. We chose source terms which are predicted by theory and PIC simulations and used scaling laws to get the corresponding parameter values at 10 PW, and source terms which have already been measured at 1 PW, in an atempt to cover a wider range of energies and typical energy/spatial distributions. Parallel computations by two of the most widely used Monte Carlo radiation transport codes - FLUKA and GEANT4 allowed for a successful cross-check of the simulations results.

"All particle" fluences were also retrieved, their distribution being meaningful for the physical processes which are expected to generate secondaries. Usually these are responsible for the radioprotection problems, as the primary beam can be more or less easily stopped in beamdumps. We also calculated the secondaries energy spectra in order to be able to compare the radiological effects of the selected electron sources at the same position in space, after specific interactions with the same medium.

We showed that the level of maximum energy by itself (or the energy distribution) does not determine univoquely the total radiation dose. Similarly, the spatial distribution is just another factor (very important however) which decides the doses given by one source term or another. Our calculations confirm that correct predictions of Monte Carlo codes rely entirely on a good definition of the source terms, and this should be a matter of careful consideration where radiation protection issues are concerned. In future, we will use our typical electron source terms implemented in FLUKA and GEANT4 within this particular study for a radiological characterization of a real laser accelerator experimental facility.

Acknowledgement

This work was supported by a grant in the programme: CAPACITIES/RO-CERN, project type: ELI-NP, E/04 HHGDE, project number 04/27.06.2014.

REFERENCES

[1]. *N.V. Zamfir,* Nuclear Physics with 10PW laser beams at Extreme Light Infrastructure – Nuclear Physics (ELI–NP), Eur. Phys. J. Special Topics, vol 223, 2014, pp. 1221-1227

[2]. *S.P. Hatchett, C.G. Brown, T..E. Cowan, E.A. Henry, J.S. Johnson, M.H. Key, J.A. Koch, A.B.Langdon, B.F. Lasinski, R.W. Lee, A.J. Mackinnon, D.M. Pennington, M.D. Perry, T.W. Phillips, M.Roth, et al.,* Electron, photon, and ion beams from the relativistic interaction of Petawatt laser pulses with solid targets. Phys. Plasmas, vol. 7, 2000, pp. 2076-2082

[3]. *D. L. Balabanski, G. Cata-Danil, D. Filipescu, S. Gales, F. Negoita , O. Tesileanu, C. A. Ur, I. Ursu, N. V. Zamfir*, Towards experiments at the new ELI-NP facility, EPJ Web of Conferences, vol. 78, 2014, pp. 06001-06007

[4]. *H.-P. Schlenvoigt, O. Jäckel, S. M. Pfotenhauer, M.C. Kaluza,* Laser-based Particle Acceleration, Advances in Solid State Lasers Development and Applications, Mikhail Grishin (Ed.), 2010

[5]. *T. Tajima, J.M. Dawson,* Laser Electron Accelerator, Phys. Rev. Lett., vol. 43, no.4, 1979, pp. 267-270

[6]. *E. Esarey, P. Sprangle, J. Krall, A. Ting,* Overview of plasma-based accelerator Concepts, IEEE Transactions on Plasma Science, vol. 24, no. 2, 1995, pp. 252–288

[7]. *C. Gahn, G.D. Tsakiris, A. Pukhov, J. Meyer-ter-Vehn, G. Pretzler, P.G. Thirolf, K.J. Witte, D. Habs,* Multi-MeV Electron Beam Generation by Direct Laser Acceleration in High-Density Plasma Channels, Phys. Rev. Lett., vol. 83, 1999, pp. 4772-4775

[8]. *X. Wang, R. Zgadzaj, N. Fazel, Z. Li, S. A. Yi, X. Zhang, W. Henderson, et al.* Quasi-monoenergetic laser-plasma acceleration of electrons to 2 GeV, Nat. Commun.4:1988 doi: 10.1038/ncomms2988, 2013

[9]. *W. Lu, M. Tzoufras, C. Joshi,* Generating multi-GeV electron bunches using single stage laser wakefield acceleration in a 3D nonlinear regime, Phys. Rev. ST Accel. Beams 10, 2007, pp. 061301-061323

[10]. *P. E. Masson-Laborde, M. Z. Mo, A. Ali, S. Fourmaux, P. Lassonde, J. C.Kieffer, W.Rozmus, D. Teychenné, R. Fedosejevs*, GeV electrons due to a transition from laser wakefield acceleration to plasma wakefield acceleration, arXiv preprint arXiv:1408.2494, 2014

[11]. *Y. Hayashi, A. Fukumi, K. Matsukado, M. Mori, H. Kotaki, M. Kando, L. M. Chen, I. Daito, S. Kondo, S. Kanazawa, A. Yamazaki1, K. Ogura, M. Nishiuchi, M. Kado, A. Sagisaka, S. Nakamura, Z. Li, S. Orimo, T. Homma, H. Daido,* Estimation of photon dose generated by a short pulse high power laser, Radiat. Prot. Dosim., vol. 121, no. 2, 2006, pp. 99–107

[12]. *T. Liang, J. Bauer, M. Cimeno, A. Ferrari, E. Galtier, E. Granados, J. Liu, B. Nagler, A. Prinz, S. Rokni, H. Tran, M. Woods,* Measurements of High-Intensity Laser Induced Ionizing Radiation at SLAC, Proceedings of SATIF-12 Fermi National Accelerator Laboratory Batavia, IL USA, April 28-30, 2014

[13]. *R. Allott, P. Wright, C.Danson, C. Edwards, D. Neely, P. Norreys, D. Rodkiss, B. Wyborn,* Vulcan Petawatt Upgrade: the radiological perspective, Central Laser Facility Annual Report 1999/2000 (CLRC Rutherford Appleton Laboratory, UK), pp.177–179 (2000).

[14]. *F. Borne, D. Delacroix, J.M. Gele, D. Masse, F. Amiranoff,* Radiation protection for an ultra-high intensity laser. Radiat. Prot. Dosim. vol. 102, no.1, 2002, pp. 61–70

[15]. ELI - Extreme Light Infrastructure WHITEBOOK, Science and Technology with Ultra-Intense Lasers, Editors G.A. Mourou, G. Korn, W. Sandner, J.L. Collier Editors, at THOSS Media GmbH, (2011), http://www.eli-beams.eu/wp-content/uploads/2011/08/ELI-Book_neues_Logo-edited-web.pdf

[16]. *A. Ferrari, P.R. Sala, A. Fasso`, J. Ranft,* FLUKA: a multi-particle transport code" CERN-2005-10, 2005, INFN/TC_05/11, SLAC-R-773

[17]. *T.T. Böhlen, F. Cerutti, M.P.W. Chin, A. Fassò, A. Ferrari, P.G. Ortega, A. Mairani, P.R. Sala, G. Smirnov, V. Vlachoudis,* The FLUKA Code: Developments and Challenges for High Energy and Medical Applications, Nuclear Data Sheets vol. 120, 2014, pp. 211-214

[18]. *V.Vlachoudis,* FLAIR: A Powerful But User Friendly Graphical Interface For FLUKA, Proc. Int. Conf. on Mathematics, Computational Methods & Reactor Physics (M&C 2009), Saratoga Springs, New York, 2009

[19]. *S. Agostinelli, J. Allison, K. Amako, J. Apostolakis, H. Arauho, et al*. (GEANT4 Collaboration) Geant4: a simulation toolkit. Nucl. Instr. Methods, A506, 2003, pp. 250-303; Web site: http://geant4.cern.ch